Journal of the European Ceramic Society 22 (2002) 403–409

www.elsevier.com/locate/jeurceramsoc

Effect of pore clustering on the mechanical properties of ceramics

R.A. Dorey[1], J.A. Yeomans*, P.A. Smith

School of Mechanical and Materials Engineering, University of Surrey, Guildford, Surrey GU2 7XH, UK

Received 23 August 2000; received in revised form 30 March 2001; accepted 3 April 2001

Abstract

The reduction in strength and, to a lesser extent, Young's modulus with increased amounts of discrete pores is frequently greater than that predicted by models based on a homogenous pore distribution. The effect of pore distribution has been examined in the present work by producing samples containing a non-homogenous distribution of pores and comparing the results with data reported for samples containing homogenously distributed pores. Young's modulus and, to a greater extent, strength were shown to have stronger dependencies on the porosity content than would be predicted for homogeneous samples. By considering the material as a composite consisting of a pore-rich continuous phase containing a dispersion of pore-free material, various models were used to predict behaviour. It was found that the strength of the material is likely to be governed by the properties of the continuous phase, while the Young's modulus is a function of the properties of the two phases, with the porous phase being described by the Spriggs equation. The implications of the different dependencies of strength and Young's modulus in terms of the resistance to crack propagation following a thermal shock were then considered. Predictions of retained strength were in good agreement with those observed after water quenching.

Keywords: Al_2O_3; Elastic modulus; Mechanical properties; Modelling; Porosity; Strength

1. Introduction

The presence of porosity within a ceramic component will lead to a reduction in the load bearing area of the material and hence can be expected to lead to a reduction in both Young's modulus and strength. A number of empirical and semi-empirical models have been proposed to describe the manner in which the mechanical properties vary with the level of porosity. One of the most commonly used forms of equation describes the effect of porosity on mechanical property as:

$$X = X_0 \exp(-bVf_P) \quad (1)$$

where X is the mechanical property, Vf_P is the volume fraction of porosity, b is an empirical constant and the subscript 0 indicates zero porosity. Eq. (1) was originally proposed by Duckworth[1] to describe the effect of porosity on strength following experimental work by Rysckewitch.[2] It was later adopted by Spriggs[3] for use in describing the effect of porosity on Young's modulus and has become known as the Spriggs equation. Other empirical and semi-empirical models to describe the effect of porosity on mechanical properties have also been proposed.[4–7] Over a limited range of porosity (typically less than 20%) the different models exhibit little variation. For the purposes of this study Eq. (1) will be utilised, due to its simplicity and the availability of data relating to it. Table 1 shows the results obtained from a number of studies of the effect of isolated pores on the strength and Young's modulus of ceramic materials in terms of b_E, the constant in the Young's modulus version of Eq. (1) and b_σ, the constant in the strength version of Eq. (1). From Table 1 it can be seen that the Young's modulus as a function of porosity shows a lower degree of variation in comparison to the dependence of strength on porosity content.

A number of theoretical models have also been developed to describe the behaviour of ceramic bodies containing a uniform distribution of pores.[6,7,11–13] Of the models proposed, the minimum solid area model[11] offers the best agreement with experimental studies. The

* Corresponding author.
E-mail address: j.yeomans@surrey.ac.uk (J.A. Yeomans).
[1] Current address: School of Industrial and Manufacturing Science, Cranfield University, Cranfield, Bedfordshire, MK43 0AL, UK.

0955-2219/02/$ - see front matter
PII: S0955-2219(01)00303-X

Table 1
Reported values of b for variation of Young's modulus and strength with porosity

Authors	Material	Type of porosity and porosity range (%)	b_E[a]	b_σ
Ali et al. (1967)	Glass	Isolated pores 1–35		2.8[b]
Biswas (1976)	Lead-zircon-titanate	Isolated pores	2.6[b]	3.4[b]
Chen[9] (1999)	Alumina	Isolated pores 0–50	~2.7	~2.7
Coble and Kingery (1956)	Alumina	Isolated pores 10–37	2.73[c], 2.8[e]	4[d]
Hasselman et al. (1964)	Glass	Isolated pores	2.1[b]	
Ryshewitch (1953)[2]	Zirconia	Isolated pores		7[d]
Wallace (1976)	Alumina	Isolated pores 2–12		2.5–2.9[b]

[a] Where two values of b_E are given they relate to analysis of the data by different investigators.
[b] Reported by Rice.[8]
[c] Reported by Spriggs.[3]
[d] Reported by Knudsen.[7]
[e] Reported by Knudsen.[10]

model describes the effect of porosity such that the mechanical property is controlled by the minimum solid area of the system. Comparison of Eq. (1) with the predictions of the model suggests a value for b of 2.6 for isolated spherical pores (for Vf_P between 0 and 0.2). From the results shown in Table 1 it can be seen that values of b_E are closer than those of b_σ to the prediction of the minimum solid area model.

A lack of detailed knowledge of the microstructures of the samples in the studies referred to in Table 1 prohibits definitive statements about the effect of pore distribution. Samples prepared using techniques likely to result in homogenous pore distributions, however, exhibit b values closer to those predicted than samples produced using techniques where thorough blending is more difficult. To examine the effect of pore distribution more closely samples containing a deliberate pore-distribution inhomogeneity were produced and tested. The results obtained from this study were then compared with results obtained from samples containing more homogenous pore distributions.[9]

2. Experimental procedure

2.1. Processing

Commercially available alumina powder (AKP 30, Sumitomo Chemical Co., Japan) with a mean particle size as determined by laser diffraction (Malvern Master Sizer) of approximately 0.5 μm and starch powder (Potato Starch, Sigma-Aldrich, UK) with a mean particle size of 15 μm were used in this study. Porous bodies of alumina were produced using a two stage process. The alumina powder was initially mixed with 20,000 molecular weight polyethylglycol binder and water using a mass ratio of 25:1:25. The resultant slurry was blended for 1 h and then dried at 75°C for 24 h. The dry powder was milled for a further 1 h to break up large agglomerates and then passed through a 250 μm sieve. The level of porosity was controlled through the addition of different amounts of starch powder to the processed alumina powder. Following starch addition, the powder mix was dry mixed for 1 hour in a rotary mill to prevent dissolution of the starch particles by water. Dry mixing also ensured that the alumina agglomerates would not break up so resulting in uneven mixing of the starch and alumina particles. Test bars were fabricated by pressing 5 g of alumina/starch mix at 20 MPa in a hardened steel die. The green bodies were sintered at 1500°C for 45 min in a chamber furnace (Lenton, UK) using a ramp rate of 5°C per min and furnace cooling.

2.2. Mechanical testing

Following sintering, the samples were ground to produce specimens of width 4.0 ±0.13 mm, thickness 3.0 ±0.13 mm and a length in excess of 45 mm in accordance with ASTM C 1161-90.[14] Samples were ground to shape using a diamond embedded grinding wheel attached to a flat bed grinder. The test samples were ground longitudinally such that no more than 0.03 mm of material was removed per pass. Final grinding and polishing of the tensile surface was conducted to 1 μm to eliminate surface defects. To reduce the risk of sample failure initiating from an edge, these were chamfered at 45° using a 10 μm polishing wheel.

Strength and Young's modulus data were obtained by loading the test samples in 3 point bending using a major span of 40 mm. To prevent possible surface defect effects, the samples were tested such that the polished surface was subjected to tensile forces during the flexure test. Machine stiffness was eliminated by directly measuring sample deflection using an extensometer mounted between the central roller support and the base of the bend rig. During testing the samples were loaded to failure using a cross-head speed of 0.5 mm/min.

Sample dimensions were measured following testing to prevent strength limiting flaws from being introduced prior to testing. Width and thickness values were taken as the mean of the values measured on either side of the point of failure. Eqs. (2) and (3) were used to determine strength (σ_f) and Young's modulus (E) values from load-displacement curves and sample dimension measurements.[14,15]

$$\sigma_f = \frac{3P_{max}L_B}{2bd^2} \tag{2}$$

$$E = \frac{P}{\delta}\frac{L_B^3}{4bd^3} \tag{3}$$

where P_{max} is applied load at failure, L_B is the span between the bottom two rollers, b and d are specimen cross-section width and thickness respectively and P/δ is the slope of the linear section of the load-displacement curve.

2.3. Microstructural characterisation

The volume fraction of porosity present within the samples was calculated from density measurements obtained using the Archimedes' technique:

$$Vf_P = 1 - \rho/\rho_0 \tag{4}$$

where ρ is the density of the sample containing added porosity and ρ_0 is the density of the sample containing no added porosity. By comparing the densities of samples containing added porosity with the control sample containing no added porosity, it was possible to calculate the volume fraction of added porosity. The degree of pore clustering was assessed by sectioning and polishing the samples to 1 μm. Due to the random nature of the section the area fraction of pore free material can be equated to the volume fraction of pore free material. The area of the pore free material was defined as extending to within one pore radius (~5 μm) of the pore cluster zone.

Grain size analysis was conducted using a linear intercept technique[16] where the mean grain size (GS) is given by:

$$GS = 1.56\frac{C_{eff}}{MN_{eff}} \tag{5}$$

C_{eff} is the effective length of the test line, M is the magnification and N_{eff} is the effective number of intercepts given by:

$$N_{eff} = N_{aa} + \frac{1}{2}N_{ab} \tag{6}$$

where N_{aa} is the number of intercepts with a grain–grain interface and N_{ab} is the number of intercepts with a grain–pore interface.

The mean pore size was determined by sectioning the samples and measuring the mean area of the pores. This was then used to calculate the mean pore diameter assuming a spherical pore geometry. A conversion factor was not applied to the calculated pore size as the polishing procedure tended to remove overhanging matrix material so presenting the maximum diameter for measurement.

2.4. Thermal shock testing

The effect of porosity on the resistance to crack propagation during thermal shock was examined by subjecting samples to rapid changes in temperature by water quenching from 200°C. Prior to quenching, samples were produced as described previously, placed on a metal support, heated to the desired temperature and held for 30 min to ensure thermal homogeneity. The samples were immersed simultaneously into the water bath by tilting the metal support. Following quenching, the samples were dried thoroughly at 75°C for 24 h prior to mechanical testing as described in Section 2.2.

Once a critical temperature differential has been exceeded, ceramics are prone to crack when subject to a rapid change in temperature. This leads to a reduction in strength. The greater the crack propagation following a thermal shock, the lower the value of the retained strength. The thermal shock resistance parameter R'''', given by Eq. (7), can be used to obtain an indication of the resistance to a material to crack propagation.[17]

$$R'''' = \frac{E\gamma_{eff}}{\sigma_f^2(1-\nu)} \tag{7}$$

In order to establish trends for R'''' it is necessary to have a qualitative understanding of the way in which the effective fracture energy, γ_{eff}, varies with porosity. Thus, a work of fracture term was determined. A sharp pre-crack was introduced into the tensile surface of the sample by means of a series of Vickers indentations such that the individual median/radial cracks would act as a single crack spanning the length of the sample. Samples were then tested as described in Section 2.2. and the work of fracture estimated from the area under the load-displacement curve.

3. Results of the baseline material characterisation

Fig. 1 shows a fracture surface of a porous sample containing 0.12 volume fraction of added porosity, which is indicative of the type of microstructure exhibited by all

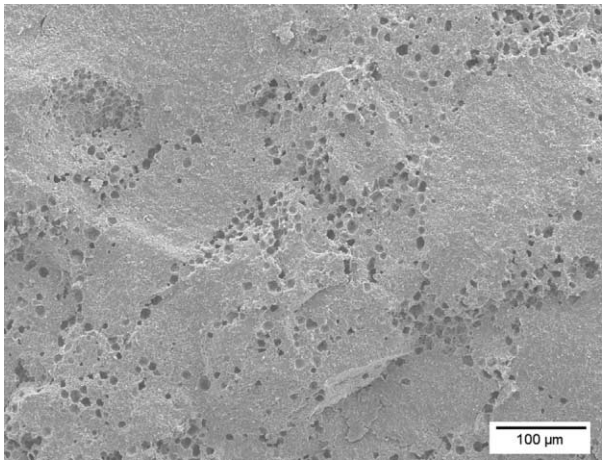

Fig. 1. Photomicrograph of fracture surface showing pore clustering resulting in variations in local volume fraction of porosity.

the materials produced from alumina/starch blends. Areas of the material appear to be free of porosity while other areas exhibit a higher concentration of pores. Hence, an inhomogenous distribution of porosity has been achieved.

Table 2 gives details of the materials produced for this study. Analysis of the microstructures showed that there was a constant degree of porosity present in the matrix phase of the samples as a result of incomplete sintering. To eliminate the effect of this porosity, all measurements of volume fraction of porosity refer to the volume fraction of deliberately added porosity such that the matrix phase is considered as a constant material (i.e. alumina with remnant porosity from the sintering process). The mean grain size of the matrix phase can be seen to be approximately constant irrespective of the degree of added porosity indicating that the presence of pores had no effect on grain growth during sintering. The constant matrix grain size enables the strength obtained from each sample set to be compared. A significant variation in grain size would lead to a variation in strength[7] which would have been superimposed onto that due to porosity thus complicating the assessment of porosity effects.

Analysis of the mean pore size shows a small degree of variation. Thus, there should be no significant size effect associated with the pores and any deviation in the properties from those predicted, based on uniformly distributed pores, can be attributed to pore clustering.

Due to the difficulty in defining the boundaries between pore clusters and matrix material, a range of values is given for the degree of pore clustering. The volume fraction of pore free material appears to vary between 0.2 and 0.5. The values arise from a series of repeat measurements of the same image and hence are a result of measurement uncertainties and not sample variations. Measurements of the volume fraction of pore free material were generally conservative and hence are likely to be underestimates of the true volume fractions. Fig. 2 demonstrates the difficulty in defining the edge of the pore clustered phase. The shaded pore free phase represents a volume fraction of 0.34, however, it can readily be seen that a different volume fraction could be obtained by redefining the boundary of the pore free phase.

4. Strength, Young's modulus and work of fracture

4.1. Results

Figs. 3, 4 and 5 show the results for strength, Young's modulus and the work of fracture term as a function of volume fraction of added porosity. It can be seen that the strength and Young's modulus decrease with increased levels of porosity and can be described accurately using the Spriggs equation such that $b_\sigma = 5.2$ and $b_E = 3.6$. The work of fracture term can be seen to increase slightly with porosity to a maximum at approximately 0.08 volume fraction of deliberately introduced porosity after which it begins to decrease again.

4.2. Difference between strength and Young's modulus behaviour

Strength and Young's modulus data for samples containing a homogenous distribution of pores has been shown to be described by a Spriggs type equation where the empirical constant, b, is equal to approximately 2.7.[9] Theoretical considerations have determined b to be approximately 2.6 over the same limited porosity range (Vf_P between 0 and 0.2). Application of the Spriggs equation to the available results for strength and

Table 2
Results of the microstructural characterisation

Density (g/cm^3)	Volume fraction of remnant porosity	Volume fraction of deliberately introduced porosity	Mean grain size (µm)	Mean pore size (µm)	Volume fraction of pore free material
3.81	0.04	0.0	2.1±0.5	–	–
3.71		0.03	2.4±0.4	14.0±0.2	0.4–0.5
3.61		0.05	2.1±0.4		0.3–0.4
3.51		0.08	2.2±0.3		0.2–0.4
3.36		0.12	2.1±0.3		0.2–0.4

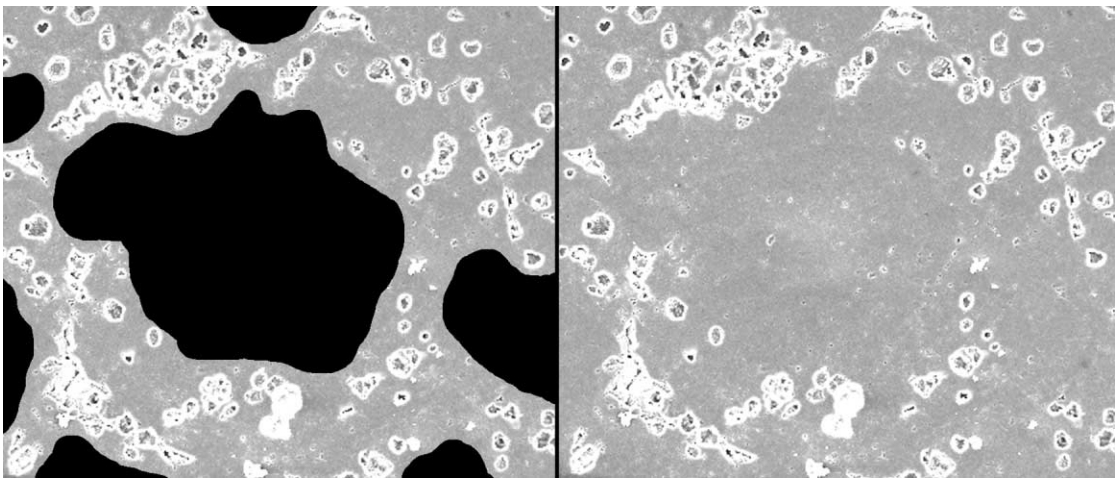

Fig. 2. Pore clustered material showing the difficulty in defining the pore free (shaded) and pore rich (unshaded) phases. The original image is included for reference.

Young's modulus (Figs. 3 and 4) results in b values of 5.6 and 3.6 respectively. Both strength and Young's modulus exhibit a porosity dependence that is greater than that predicted and observed previously in other studies.

The work conducted by Chen[9] used the same starting materials as this study. A more homogenous pore distribution, however, was produced through the use of a tape casting route. The homogenous pore distribution obtained by Chen resulted in a porosity dependence such that b_E and b_σ were both approximately equal to 2.7. Examination of the microstructures obtained during the current study clearly indicates that the pores are not distributed homogeneously (Fig. 1).

The effect of such a microstructure might be to cause the material as a whole to act as a composite composed of one phase which is pore-free dispersed in another phase which is pore-rich. The pore-free phase would be expected to exhibit the same material properties as the material with no added porosity while the pore-rich phase may exhibit a porosity dependence that could be described by a suitable model. The complex nature of the pore clustering makes exact predictions of material properties difficult. However, an approximate description of the porosity behaviour can be obtained by considering the material as a two phase composite with the porous phase as the continuous 'matrix' phase.

The bounds for the Young's modulus behaviour can be represented using the Voigt and Reuss equations given by Eqs. (7) and (8) respectively.

$$E_c = E_1 Vf_1 + E_2(1 - Vf_1) \quad (8)$$

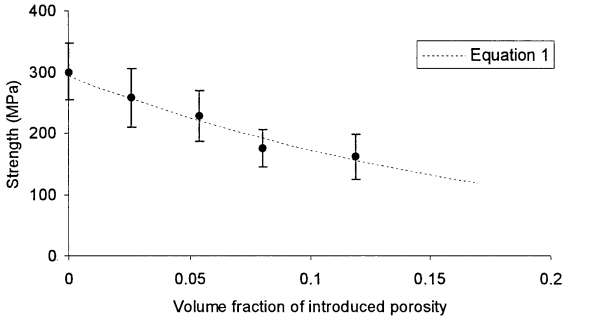

Fig. 3. Variation of strength with added porosity (at least 5 samples were used per data point with the error bars representing 1 standard deviation).

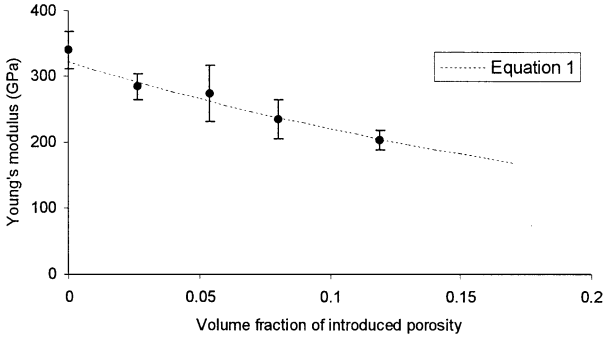

Fig. 4. Variation of Young's modulus with added porosity (at least 3 samples were used per data point with the error bars representing 1 standard deviation).

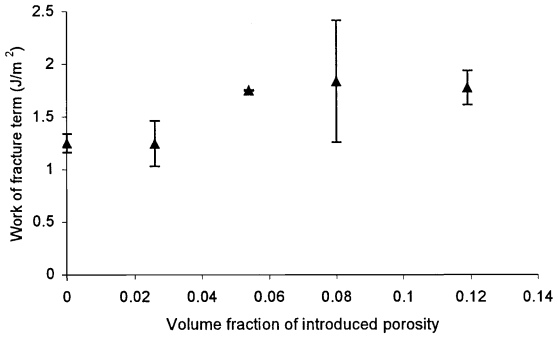

Fig. 5. Variation in work of fracture with added porosity (at least 3 samples were used per data point with the error bars representing 1 standard deviation).

$$\frac{1}{E_c} = \frac{Vf_1}{E_1} + \frac{(1 - Vf_1)}{E_2} \quad (9)$$

where subscripts C, 1 and 2 relate to the composite, phase 1 and phase 2.

Examination of the pore distributions found in the clustered porosity samples showed the volume fraction of pore free material to be in the range 0.2–0.5. Due to the difficulty in identifying the boundary of the pore clustered phase it is reasonable to assume that the true level of pore free material is likely to be towards the upper limit observed and a value of 0.5 was used for modelling purposes.

Fig. 6 shows the upper and lower bounds for a system where pore clustering results in a twofold increase in the level of local porosity (i.e. volume fraction of pore-free phase = 0.5). To construct the curves phase 1 was considered to be pore-free at all times and phase two was described using Eq. 1 with $b = 2.6$. The volume fraction of porosity within the clusters was adjusted subject to the limitation that the macroscopic volume fraction of porosity did not change. Also included in Fig. 6 are curves representing predictions for a homogenous pore distribution, obtained using Eq. (1) with $b = 2.6$, and a situation in which the weaker phase dominates, the 'weak link' curve. In the 'weak link' approach it is assumed that the entire material has the same level of porosity as the porous (continuous) phase of the equivalent two phase material.

Comparison of Eq. (1) with the predictions for the lower limit (Reuss) approximation and the 'weak link' prediction results in b values of 3.3 and 5.2 respectively which show reasonable agreement with the results obtained from experiments where $b_E = 3.6$ and $b_\sigma = 5.6$.

In reality the effect of pore clustering will be more complex as the concentration of pores within the clustered zones will not be constant throughout the cluster and different pore clusters will exhibit different degrees of clustering. The simplification presented here demonstrates that pore clustering can lead to a difference in the porosity dependence exhibited by strength and Young's modulus. From the results presented it is possible to infer that the large degree of scatter associated with b_σ values reported in literature might relate to inhomogeneous pore distributions.

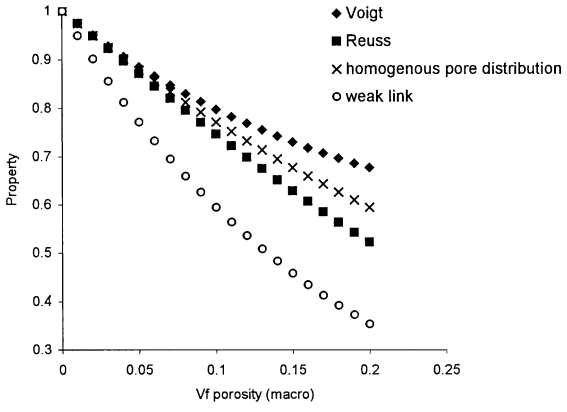

Fig. 6. Variation in porosity dependence showing homogenous pore distribution ($b = 2.6$), upper and lower bounds for Young's modulus and the weak link (behaviour of weakest phase) representative of the strength dependence.

5. Effect of pore clustering on thermal shock resistance

The more marked decrease in strength for a material in which the pores are clustered, rather than homogeneously distributed, could lead to a greater resistance to crack propagation following a thermal shock and hence a higher value of relative retained strength i.e. strength following quenching normalised by strength before quenching. Fig. 7 shows the predicted resistance to crack propagation (R'''') for both a clustered and a homogenous pore distribution. The pore clustering data were obtained from the work conducted in this study while the homogenous pore distribution data were obtained from work by Chen.[9]

The resistance parameter R'''' describes the resistance to crack propagation and hence should indicate the degree by which the resultant crack length will change (i.e. a two-fold increase in resistance parameter should result in a two-fold decrease in crack length). The resultant strength can be estimated if it is assumed that strength is proportional to the square root of the crack size. Table 3 gives values for R'''', estimates of the relative retained strengths and the measured values following a 200°C water quench. All the values have been normalised by the strength reductions for the material containing no deliberately introduced porosity.

It can be seen from Table 3 that both the predicted and observed values of retained strength show an increase with increased levels of porosity. The observed improvements are generally very close to those predicted. Further, it is suggested that clustered pores are likely to be more beneficial than homogeneously distributed pores, in terms of resisting crack propagation following a thermal shock.

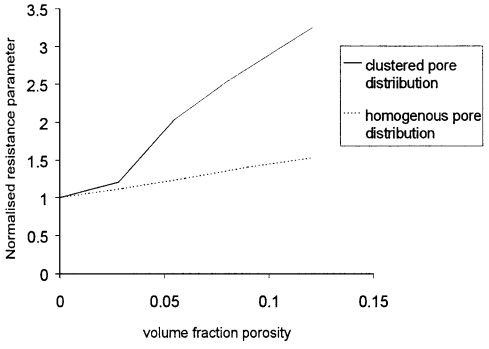

Fig. 7. Predicted resistance to crack propagation (R'''') for clustered and homogenous pore distributions.

Table 3
Comparison of predicted and measured relative retained strength following a 200°C water quench

	Normalised R''''	Retained strength ($\Delta T = 200°C$)/initial strength	
Vf_p		Predicted	Measured
0.00	1.00	–	0.20
0.03	1.21	0.22	0.22
0.05	2.04	0.29	0.29
0.08	2.54	0.32	0.38
0.12	3.25	0.36	0.40

6. Concluding remarks

Strength and Young's modulus values have been obtained from a series of samples containing different volume fractions of non-homogeneously distributed pores. It was shown that the decrease in strength and Young's modulus was greater than that expected for samples containing a homogenous pore distribution, with strength showing the greater dependence on the porosity content.

A simplified model was proposed in which the material was considered to be a composite consisting of a continuous pore-rich phase containing a dispersion of pore-free material. On the basis of microstructural studies, 50% of the material was considered to be pore-free. The strength of the body was best estimated by assuming that it was controlled by the continuous phase while the Young's modulus was found to be a function of both the pore-free and pore-rich phases, with the behaviour of the pore-rich phase being described by the Spriggs equation.

The implications of the different strength and Young's modulus behaviour as a function of porosity for resistance to crack propagation during thermal shock were investigated. Good agreement was obtained between predictions of retained strength and those obtained in practice. It is concluded that pore clustering may be beneficial in terms of retained strength following a thermal shock.

References

1. Duckworth, W., Discussion of Ryshkewitch paper by Winston Duckworth. *J. Am. Ceram. Soc.,* 1953, **36**, 68.
2. Ryshkewitch, E., Compression strength of porous sintered alumina and zirconia. *J. Am. Ceram. Soc.,* 1953, **36**, 65–68.
3. Spriggs, R. M., Expression for effect of porosity on elastic modulus of polycrystalline refractory materials, particularly aluminium oxide. *J. Am. Ceram. Soc.,* 1961, **44**, 628–629.
4. Phani, K. K. and Niyogi, S. K., Young's modulus of porous brittle solids. *J. Mater. Sci.,* 1987, **22**, 257–263.
5. Hasselman, D. P. H., On the porosity dependence of the elastic moduli of polycrystalline refractory materials. *J. Am. Ceram. Soc.,* 1962, **45**, 452–453.
6. Rossi, R. C., Prediction of the elastic moduli of composites. *J. Am. Ceram. Soc.,* 1968, **51**, 433–439.
7. Knudsen, F. P., Dependence of mechanical strength of brittle polycrystalline specimens on porosity and grain size. *J. Am. Ceram. Soc.,* 1959, **42**, 376–387.
8. Rice, R. W., *Porosity of Ceramics*. Marcel Dekker, ISBN:0-8247-0151-8, 1998.
9. Chen, Y., Thermal Shock Behaviour of Ceramics with Porous and Layered Structures, PhD thesis, University of Cambridge, 1999.
10. Knudsen, F. P., Effect of porosity on Young's modulus of alumina. *J. Am. Ceram. Soc.,* 1962, **45**, 94–95.
11. Rice, R. W., Comparison of stress concentration versus minimum solid area based mechanical property-porosity relations. *J. Mater. Sci.,* 1993, **28**, 2187–2190.
12. Wang, J. C., Young's modulus of porous materials Part 1 theoretical derivation of modulus-porosity correlation. *J. Mater. Sci.,* 1984, **19**, 801–808.
13. Ramakrishnan, N. and Arunachalam, V. S., Effective elastic moduli of porous ceramic materials. *J. Am. Ceram. Soc.,* 1993, **76**, 2745–2752.
14. ASTM Designation: C 1161-90, Standard test method for flexural strength of advanced ceramics at ambient temperature.
15. ASTM Designation: C 674-88, Standard test methods for flexural properties of ceramic whiteware materials.
16. Wurst, J. C. and Nelson, J. A., Linear intercept technique for measuring grain size in two-phase polycrystalline ceramics. *J. Am. Ceram. Soc.,* 1972, **55**, 109.
17. Hassleman, D. P. H., Elastic energy at fracture and surface energy as design criteria for thermal shock. *J. Am. Ceram. Soc.,* 1963, **46**, 535–540.